J. Fluid Mech. (1987), *vol.* 184, *pp.* 75–99
Printed in Great Britain

Generation of upstream advancing solitons by moving disturbances

By T. YAO-TSU WU
Division of Engineering and Applied Science, California Institute of Technology, Pasadena, CA 91125, USA

(Received 27 March 1986 and in revised form 14 April 1987)

This study investigates the recently identified phenomenon whereby a forcing disturbance moving steadily with a transcritical velocity in shallow water can generate, periodically, a succession of solitary waves, advancing upstream of the disturbance in procession, while a train of weakly nonlinear and weakly dispersive waves develops downstream of a region of depressed water surface trailing just behind the disturbance. This phenomenon was numerically discovered by Wu & Wu (1982) based on the generalized Boussinesq model for describing two-dimensional long waves generated by moving surface pressure or topography. In a joint theoretical and experimental study, Lee (1985) found a broad agreement between the experiment and two theoretical models, the generalized Boussinesq and the forced Korteweg–de Vries (fKdV) equations, both containing forcing functions. The fKdV model is applied in the present study to explore the basic mechanism underlying the phenomenon.

To facilitate the analysis of the stability of solutions of the initial-boundary-value problem of the fKdV equation, a family of forced steady solitary waves is found. Any such solution, if once established, will remain permanent in form in accordance with the uniqueness theorem shown here. One of the simplest of the stationary solutions, which is a one-parameter family and can be scaled into a universal similarity form, is chosen for stability calculations. As a test of the computer code, the initially established stationary solution is found to be numerically permanent in form with fractional uncertainties of less than 2% after the wave has traversed, under forcing, the distance of 600 water depths. The other numerical results show that when the wave is initially so disturbed as to have to rise from the rest state, which is taken as the initial value, the same phenomenon of the generation of upstream-advancing solitons is found to appear, with a definite time period of generation. The result for this similarity family shows that the period of generation, T_s, and the scaled amplitude α of the solitons so generated are related by the formula $T_s = \text{const}\,\alpha^{-\frac{3}{2}}$. This relation is further found to be in good agreement with the first-principle prediction derived here based on mass, momentum and energy considerations of the fKdV equation.

1. Introduction

This paper is a continued study of the intriguing phenomenon whereby a forcing disturbance moving steadily with a transcritical velocity in shallow water can generate, continuously and periodically, a succession of solitary waves, propagating ahead of the disturbance in procession, while a train of weakly dispersive waves develop behind the disturbance. This phenomenon was discovered first numerically, with its physical significance identified for the case of plane motions by Wu & Wu (1982) using the generalized Boussinesq model proposed by Wu (1979, 1981). Experimentally, this phenomenon was investigated by Huang *et al.* (1982) and by Sun (1985) for ship models moving in a towing tank with various transcritical speeds. A striking feature of the ship-model test is that the unsteady waves emerging successively to propagate ahead of a steadily moving three-dimensional ship model are invariably two-dimensional, spanning straight across the channel. Behind the ship model, one finds the three-dimensional wave pattern more commonly seen. Calculations were performed by Ertekin (1984) and Ertekin, Webster & Wehausen (1985) who employed Green–Naghdi's directed-sheet model for numerical solutions to two-dimensional problems with similar results, which were used for qualitative comparison with ship-model experiments. The plane-flow case was also evaluated by Akylas (1984) and Cole (1985) based on the Korteweg–de Vries model with a singular forcing function, yielding similar qualitative results. Subsequently, this problem was analysed by Grimshaw & Smyth (1986) and Smyth (1986) applying the modulation theory of Whitham (1965, 1974).

For the case of plane flow, a combined numerical and experimental study was carried out by Lee (1985) with a two-dimensional cambered topography moving along the horizontal floor of a water layer. The experimental results were predicted, with a broad agreement, by the corresponding numerical results of both the generalized Boussinesq and forced Korteweg–de Vries models. According to Lee, the agreement is especially satisfactory, when the depth Froude number ($F = U/(gh_0)^{\frac{1}{2}}$, U being the constant velocity of the forcing disturbance, g the gravitational acceleration, and h_0 the initial uniform water depth) is nearly of the critical value of unity and when the camber-height to water-depth ratio is appropriately small.

Various attempts have been made to extend the two-dimensional formulation to a three-dimensional one. Mei (1986) derived an inhomogeneous KdV equation to analyse a slender ship hull and obtained upstream-propagating solitary waves. The problem of a three-dimensional surface-pressure distribution (simulating a ship hull) moving in a channel was evaluated numerically by Ertkin, Webster & Wehausen (1986) based on the Green–Naghdi directed-sheet model and by Wu & Wu (1987) who used the generalized Boussinesq equations. Recently, Katsis & Akylas (1987) calculated some three-dimensional long waves bounded by sidewalls using the Kadomtsev–Petviashvili equation.

Historically, various aspects of this phenomenon seem to have been encountered earlier by several observers. The very first solitary wave, reported by John Scott Russell, that emerged and surged ahead from a boat suddenly stopped in a narrow canal might well be relevant. In a series of towing-tank tests of ship models in shallow water, this phenomenon was observed fifty years ago by Thews & Landweber (1935, 1936), and was rediscovered, independently, with a new understanding by Huang *et al.* (1982) and Sun (1985). Aside from involving a Galilean transformation and some rather secondary effects such as the viscous boundary-layer growth, two closely related phenomena of upstream-propagating nonlinear waves and hydraulic jumps caused by external disturbances in recirculating water channels were observed by Favre (1935) when water was discharged into the channel, and by Binnie & Orkney (1955) who used surface gliding plates to transfer momentum and energy. In these earlier investigations the essential significance of the phenomenon seems to have escaped full attention, perhaps owing to lack of opportunities of making clear experimental observations over a long enough time to reveal the remarkable periodicity of soliton generation in conspicuous contrast to the steadiness of a moving disturbance.

Quite clearly, similar phenomena can occur in practically all soliton-bearing physical and biological systems. A closely related case is the flow of stratified fluid over a localized topography acting as forcing function, which has been the subject of several recent studies. In a series of experiments, Baines (1977, 1984) observed upstream disturbances when the stratified flow was near a resonance. This basic problem was analysed by Grimshaw & Smyth (1986) and Smyth (1986). Also pertinent are the investigations by Patoine & Warn (1982) and by Malanotte-Rizzoli (1984) on the resonant forcing of Rossby waves by topography. Recently, a combined theoretical and experimental study of internal solitons produced by moving topography was made by Zhu (1986) and by Zhu, Wu & Yates (1986, 1987). Waves of a similar nature can also be generated by moving boundaries, as reported by Chu, Xiang & Baransky (1983) on nonlinear waves in plasma. Some analogous phenomena found in biological and other contexts have been discussed by Keller (1985).

Several aspects of the new phenomenon appear remarkable, of which the foremost is perhaps the outstanding feature that the response of such a fluid-mechanical system to a steadily moving disturbance can be unsteady when the system is in resonance and can contain a conspicuous time-periodic component. Generally speaking, its physical significance can be attributed to a well-balanced interplay between the nonlinear and dispersive effects. In this transcritical speed range, the dispersive effect is weak, so the velocity of propagating mechanical energy away (by means of radiating long waves) from the forcing disturbance is about equal to the velocity of the moving disturbance. The local wave will therefore grow as the energy acquired by local fluid at the rate of work by the moving disturbance keeps accumulating. When the local wave reaches a certain threshold magnitude, the increase in phase speed with increasing amplitude (due to the nonlinear effects) will be sufficient to make the wave break away from the disturbance, thus 'born free' as a new solitary wave propagating forward with a phase velocity appropriate to its own amplitude. The process is then repeated over a new cycle. While this physical reasoning seems adequate to explain why, it falls short of explaining how the phenomenon is manifested.

To pursue the investigation further, we might raise some stimulating questions such as: What is the basic mechanism that causes the periodic generation of solitons? Can we predict accurately, not by purely numerical methods as has been done, the period of generation of these upstream-running solitons? What is the boundary in the space of the key parameters involved that separates the regions of occurrence and non-existence of the phenomenon?

This paper is a preliminary study aimed at determining the basic mechanism underlying the phenomenon. In order to ascertain if the phenomenon is manifested owing to a nonlinear instability of stationary solution and a bifurcation into a time-periodic solution, an analysis is initiated here first to study the solutions of the initial-boundary-value problem of the forced Korteweg–de Vries (fKdV) equation, which is derived in §3. In §4, a first-principle theorem is developed based on mass, momentum and energy considerations of the fKdV equation. In §5, a family of an infinity of steadily moving forcing functions is found, each of which gives rise to a forced steady solitary wave (of permanent form) as an exact solution of the fKdV equation if the same solution existed initially. In §6, a perturbation theory is formulated for investigating the nonlinear stability of forced steady solitary waves when such a wave is given a finite perturbation. For definiteness, the perturbation is taken as arbitrary depature of the initial value of a perturbed motion from the stationary solution. Specific consideration is given to a special one-parameter family of forced solitary waves, with proper choices of forcing function and initial value so that the single parameter can be eliminated by a similarity group transformation. The solution to this perturbation problem is then determined numerically with two limiting cases of initial values. The results show that the stationary solution remains stable if the initial perturbation (depature from stationary solution) vanishes. But when the rest state is taken as the initial value, this impulsive perturbation turns out to be so strong that the same phenomenon of the generation of solitons is numerically found to appear, like that produced by arbitrary forcing functions, with a definite time period of generation. This numerical result (in similarity form) yields a set of rules which are found to be in good agreement with the first-principle prediction given in §4. It is hoped that this study will cast some light on the development of general methods for evaluating forced nonlinear waves.

2. The generalized Boussinesq model

The phenomenon of periodic generation of solitary waves by a two-dimensional disturbance moving steadily with a transcritical speed through a layer of water initially uniform in depth was numerically identified by Wu & Wu (1982) using the following pair of equations of the Boussinesq class (which is a special case of the equations derived by Wu 1979, 1981) for modelling forced two-dimensional long waves in the vertical (x, z)-plane:

$$\zeta_t + [(h+\zeta)\,u]_x = -h_t, \tag{1}$$

$$u_t + uu_x + g\zeta_x = -\frac{1}{\rho}p_{a_x} + \tfrac{1}{2}h[h_t + (hu)_x]_{xt} - \tfrac{1}{6}h^2 u_{xxt}, \tag{2}$$

where the subscripts x and t denote partial differentiation. Here x is the horizontal coordinate, t is the time, g is the gravitational acceleration pointing in the negative z-direction, $z = \zeta(x,t)$ is the free-surface elevation, $z = -h(x,t) = -h_0 + b(x,t)$ indicates a topography $b(x,t)$ which may move over the bottom floor at depth h_0 (h_0 being a constant), $u(x,t)$ is the water-layer depth-averaged x-component velocity of the fluid, ρ is the constant fluid density, and $p_a(x,t)$ is a given ambient pressure acting on the free surface. This generalized Boussinesq model is assumed to hold for weakly nonlinear and weakly dispersive long waves such that

$$\alpha = \frac{a}{h_0} \ll 1, \quad \epsilon = \left(\frac{h_0}{\lambda}\right)^2 \ll 1, \quad \alpha = O(\epsilon), \tag{3}$$

where a is a typical wave amplitude and λ is a typical wavelength. The model admits as external forcing disturbances the surface pressure $p_a(x,t)$ and topography (or 'bump') $b(x,t)$, which are supposed to be slowly varying functions such that

$$|h_x|, \left|\frac{h_t}{c_0}\right|, \frac{|p_{a_x}|}{\rho g}, \frac{|p_{a_t}|}{\rho g c_0} \leqslant O(\alpha\epsilon^{\frac{1}{2}}), \tag{4}$$

where $c_0 = (gh_0)^{\frac{1}{2}}$. With these forcing disturbances, (1) is exact while the momentum equation (2) has a relative error term (with respect to the leading term) of $O(\alpha\epsilon, \epsilon^2)$ (see Wu 1981). It is in this sense that the classical Boussinesq model, originally introduced for closed fluid-mechanical systems modelled by (1)–(3) with

$h = h_0 = \text{const.}$ and $p_a = 0$ and characterized by their initial values and by fixed boundaries, is extended in applicability to open systems which may evolve with exchange of mass, momentum and energy with some external agencies and may have moving boundaries (for exchanging momentum and energy) as prescribed forcing functions.

Since the generalized Boussinesq model still seems too complex to be used for investigating hydrodynamic stability of the fluid motion generated by a steadily moving disturbance, we now turn to explore a simpler model, which is the forced Korteweg–de Vries (fKdV) model.

3. The forced Korteweg–de Vries (fKdV) model

Like the generalized Boussinesq model, the classical KdV equation can be extended to admit arbitrary forcing functions if the forcing disturbances are limited to unidirectional motion, say

$$p_a = p_a(x+Ut), \quad b = b(x+Ut), \tag{5}$$

representing a left-going (or right-going) surface pressure and topography when U is positive (or negative). These forcing functions are supposed to be sufficiently smooth, localized, square-integrable in $x(-\infty, \infty)$, and to vanish identically for $t < 0$. We further assume that the constant U is nearly critical so that the depth Froude number

$$F = \frac{U}{c_0} = 1 + \epsilon\delta_F, \quad (c_0 = (gh_0)^{\frac{1}{2}}), \tag{6}$$

where $\delta_F = O(1)$ is a detuning parameter measuring how close the flow is to resonance (which by linear theory is when $\delta_F = 0$).

To deal with this class of weakly forced motions, we adopt the stretched coordinates

$$\xi = \epsilon^{\frac{1}{2}} x_*, \quad \tau = \epsilon^{\frac{3}{2}} t_*, \tag{7a}$$

$$x_* = \frac{x+Ut}{h_0}, \quad t_* = \frac{c_0 t}{h_0}, \tag{7b}$$

and we assume the following asymptotic expansions for $f = u_*, \zeta_*, p_{a*}$, and b_*:

$$f(x,t;\epsilon) = \epsilon f_1(\xi,\tau) + \epsilon^2 f_2(\xi,\tau) + O(\epsilon^3), \tag{8a}$$

where
$$u_* = \frac{u}{c_0}, \quad \zeta_* = \frac{\zeta}{h_0}, \quad p_{a*} = \frac{p_a}{\rho c_0^2}, \quad b_* = \frac{b}{h_0}. \tag{8b}$$

Here x_* is the coordinate fixed in the body frame of reference (i.e. moving with the surface pressure or the topography) and τ is a slow time. Substituting (7) and (8) in (1) and (2), with $h = h_0 - b(x,t)$, we obtain for the first-order terms the equations

$$\frac{\partial}{\partial \xi}[\zeta_1 + u_1 - b_1] = 0, \tag{9}$$

$$\frac{\partial}{\partial \xi}[\zeta_1 + u_1 + p_{a1}] = 0, \tag{10}$$

Upon integration of (9) and (10) from the rest state at infinity, it follows that

$$\zeta_1 = -u_1, \tag{11}$$

$$p_{a1} = 0, \quad b_1 = 0. \tag{12}$$

The last two compatibility conditions on p_a and b are necessary for the solvability of ζ_1 and u_1 if both p_a and b are to be arbitrary as assumed. The second-order terms in (1) and (2) then give, with use of (12),

$$\frac{\partial}{\partial \tau}\zeta_1+\frac{\partial}{\partial \xi}[\zeta_2+u_2-b_2+\zeta_1 u_1+\delta_F \zeta_1] = 0, \tag{13}$$

$$\frac{\partial}{\partial \tau}u_1+\frac{\partial}{\partial \xi}[\zeta_2+u_2+p_2+\tfrac{1}{2}u_1 u_1-\delta_F u_1-\tfrac{1}{3}u_{1\xi\xi}] = 0. \tag{14}$$

From these equations the second-order variables can be eliminated to yield, with use of (11), an evolution equation for ζ_1, which can be immediately recast for $\zeta_*(x_*, t_*)$ as

$$\zeta_t+[(F-1)-\tfrac{3}{2}\zeta]\,\zeta_x-\tfrac{1}{6}\zeta_{xxx} = \tfrac{1}{2}(p_a+b)_x, \tag{15}$$

where all the variables and the forcing functions are understood to assume the dimensionless form (see (7*b*), (8*b*)), now with the $*$ omitted. This is the forced Korteweg–de Vries (fKdV) equation, which is seen to hold with a relative error term of $O(\epsilon^2)$. To the same order of expansion, the sum of (13) and (14) yields a relationship between u and ζ as

$$u = -(\zeta-\tfrac{1}{4}\zeta^2)-\tfrac{1}{6}\zeta_{xx}-\tfrac{1}{2}(p_a-b). \tag{16}$$

In dimensional form, (15) becomes

$$\frac{1}{c_0}\zeta_t+\left[\left(\frac{U}{c_0}-1\right)-\frac{3}{2}\frac{\zeta}{h_0}\right]\zeta_x-\tfrac{1}{6}h_0^2\,\zeta_{xxx} = \frac{1}{2}\left(\frac{p_a}{\rho g}+b\right)_x. \tag{17}$$

This equation holds for left-going (or right-going) waves when U and c_0 are both positive (or both negative), which amounts to having the sign changed for the term with ζ_t in (15) and for that with u in (16) for the case of right-going disturbances.

Mathematically, we should note that in the absence of forcing, the classical KdV equation is completely integrable (see Gardner *et al.* 1967; Whitham 1974; Miles 1980; Dodd *et al.* 1982). In the presence of forcing, the fKdV equation is not known to be integrable, and solutions can be obtained only by numerical and perturbation techniques. And, similar to the uniqueness proof for the KdV equation (see Lax 1968), the solution of the fKdV equation can be shown under certain conditions to be uniquely determined given the forcing functions and the initial value; a proof is given in the Appendix.

We further note that the first-order compatibility condition of the fKdV model requires the forcing functions p_a and b to be of $O(\epsilon^2)$ by virtue of (12), a requirement that is stronger than (4) assumed for the generalized Boussinesq model. Further, for the fKdV model, the surface pressure p_a and topography b are seen from (15) to be entirely equivalent (in their dimensionless form), whereas for the generalized Boussinesq model there exists some, though rather mild, differentiation between them. In practical application, the fKdV model therefore implies that the resulting motion induced by a horizontally moving thin body would not depend on the body's depth of submergence.

The refined differences between the two theoretical models have been investigated by Lee (1985) in a joint theoretical and experimental study. The moving disturbances used for numerical computation (which was carried out with reference to the fluid frame) assume the distribution

$$P(x,t) = \tfrac{1}{2}P_m\left[1+\cos\frac{2\pi}{L}(x+Ut)\right] \quad (-\tfrac{1}{2}L < (x+Ut) < \tfrac{1}{2}L), \tag{18}$$

and $P = 0$ elsewhere, where $P(x, t)$ represents $p_a/\rho g h_0 + b/h_0$, and P_m is a constant. The motion is assumed to start impulsively with the initial conditions

$$\zeta(x,0) = -h_0 P(x,0), \quad u(x,0) = 0, \tag{19a}$$

$$\zeta(x,0) = 0, \quad u(x,0) = 0, \tag{19b}$$

for the surface pressure and floor topography modes, respectively. This initial-value problem has been solved numerically over a transcritical speed range†. The numerical method developed by Wu & Wu (1982) and later made more efficient by Lee (1985) is based on the modified Euler's predictor–corrector algorithm in advancing time and the central-difference approximation for the space derivatives. A mixed implicit–explicit scheme is adopted for the forward-difference computation of ζ and u, the implicit part being incorporated in order to achieve the desired numerical stability and accuracy with a relatively large time-step Δt ($O(10^{-1})$ in dimensionless form). As an effective 'open-boundary condition' for the two boundaries of the computation region use has been made of the empirical equation

$$Q_t \pm c_0 Q_x = 0, \tag{20}$$

where $Q = \zeta$ and u, and the + and − signs are for the downstream and upstream boundaries, respectively, so as to guide the wave to leave the region of computation at the rate of linear phase velocity $c_0 = (gh_0)^{\frac{1}{2}}$. This condition was found to be so effective that it can maintain the boundaries almost free of non-physical reflections (leaving only some minute residual reflection with a relative error of $O(10^{-3})$ or less due to various sources of imperfection) and thereby enhances the numerical stability.

The general features of the numerical results within a narrow transcritical range can be seen from the following typical examples of the fKdV model:

$$P_m = \frac{b_{max}}{h_0} = 0.2, \qquad h_0 = 1, \quad L = 2, \quad F = 1.0; \tag{21}$$

$$P_m = \frac{b_{max}}{h_0} = -0.2, \quad h_0 = 1, \quad L = 2, \quad F = 1.0. \tag{22}$$

Here (21) describes a positive surface pressure (or a bottom topography) and (22) an equal and opposite one, both assuming the same distribution given by (18), and both moving at the critical speed of $U = c_0$. The corresponding numerical results are shown in figures 1 and 2. A conspicuous feature of the result is that, after the surface pressure has been exerted and kept moving at the critical speed for a definite period of time, a solitary wave emerges just ahead of the disturbance, and eventually breaks away to propagate forward as a free solitary wave, forming an entity (rising entirely above the initial undisturbed water level) which we may call a 'precursor soliton', or a 'runaway soliton'. This is followed by another new solitary wave going through the same cycle, and this process seems to continue periodically and indefinitely.

Immediately behind the moving topography there trails an ever-longer region of depressed water, of nearly uniform depth, which is in turn followed by a train of cnoidal-like waves oscillating about the initial free-surface level, with the wave height decreasing with distance and with the train length increasing with time, and eventually merging with the undisturbed water further behind. The excess mass of

† In our calculations, as is the established practice, to ensure numerical stability (15) is replaced by the 'regularized KdV equation', which is obtained by replacing ζ_{xxx} in the dispersion term in (15) by $\zeta_{xxt} + F\zeta_{xxx}$ (see (58); and Benjamin, Bona & Mahoney 1972).

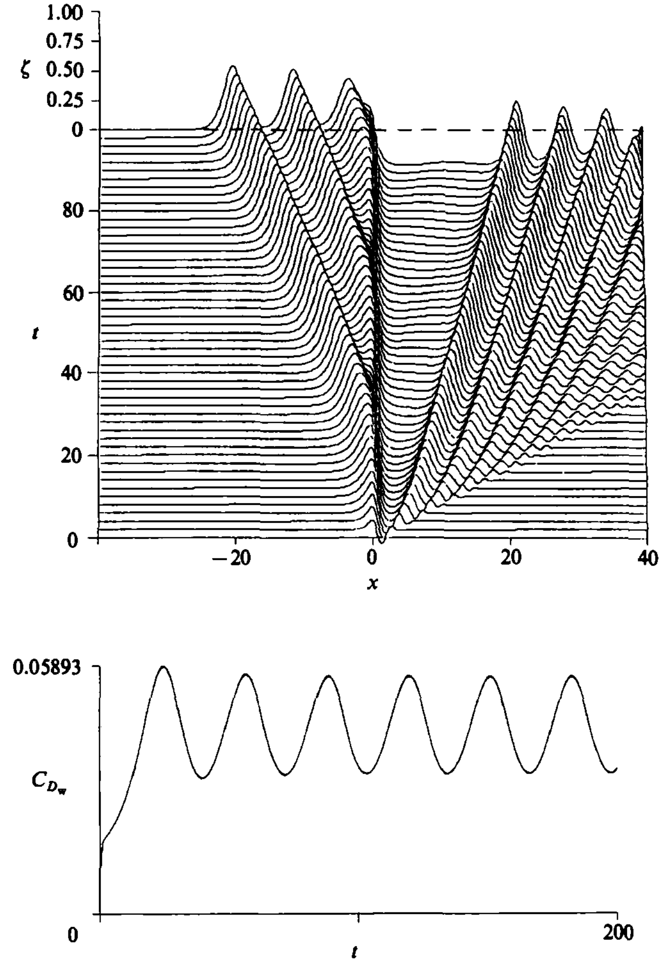

FIGURE 1. Numerical results of the forced KdV model (15) for the surface wave elevation ζ (calculated with intervals $\Delta x = 0.2$ and $\Delta t = 0.1$ and shown with an equal time increment of 2.0) and the wave resistance coefficient C_{D_w} (with asymptotic mean of $\overline{C}_{D_w} = 0.044$) due to the cosine forcing distribution (18) with positive forcing (21): $P_m = 0.2$, $L = 2.0$, and $F = 1.0$. The first three upstream-progressing solitons are generated at $t = 24.5$, 56.8 and 89.2 (the maxima of C_{D_w}), with a period of $T_s = 32.4$. ----, initial undisturbed wave surface shown as reference at $t = 100$.

the upstream-advancing solitons was found to come almost entirely from the region of surface depression.

Also shown in figure 1 is the drag (which is the resistance due to unsteady wave making) D_w experienced by the moving disturbance (per unit width) which, based on the fKdV rule of equivalence of p_a and b, is given by

$$D_w = -\int_{-\frac{1}{2}L}^{\frac{1}{2}L} p_a(x,t)\frac{\partial \zeta}{\partial x}\,\mathrm{d}x, \tag{23}$$

and has the coefficient

$$C_{D_w} = \frac{D_w}{\rho g h_0 L}. \tag{24}$$

The numerical result for C_{D_w} given in figure 1 for positive forcing shows that the drag oscillates nearly sinusoidally about a positive mean value of $\overline{C}_{D_w} = 0.044$, reaching

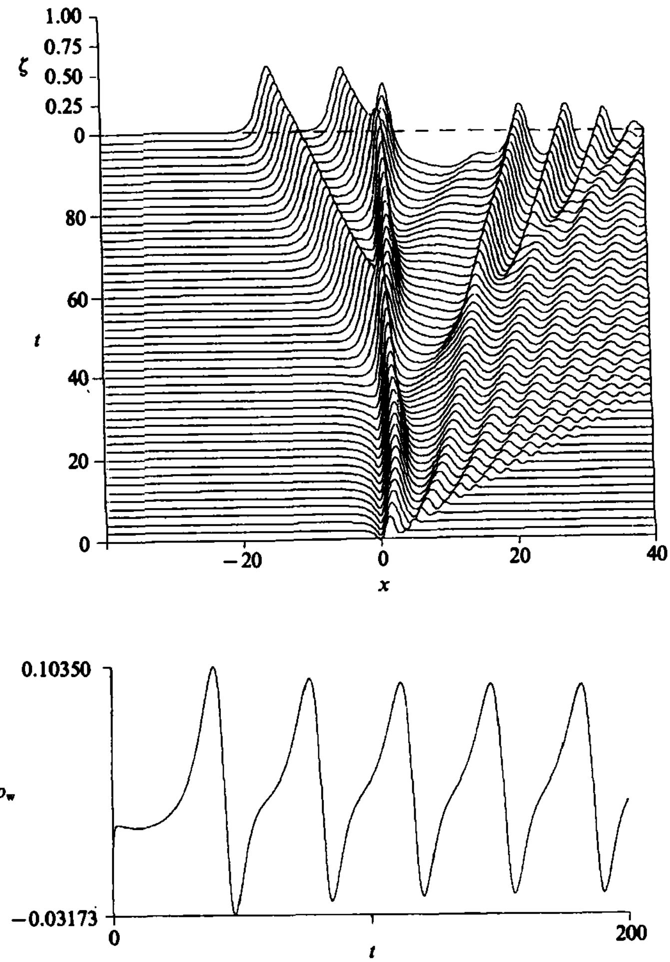

FIGURE 2. Numerical results of the fKdV model for surface elevation ζ and wave resistance coefficient C_{D_w} (with mean $\overline{C}_{D_w} = 0.036$) due to forcing distribution (18) with negative forcing (22): $P_m = -0.2$, $L = 2.0$, and $F = 1.0$. The first three upstream-progressing solitons are generated at $t = 40.8$, 75.6 and 110.4, with a period of $T_s = 34.8$. For the other symbols, see figure 1 caption.

a maximum (or minimum) when the free surface at the leading edge of the forcing disturbance is at the highest (or the lowest) elevation. The duration from the time of a minimum drag to that of the next maximum drag may be called the 'growth phase' and the remainder of the period the 'departure phase' for production of a new soliton. As the period of C_{D_w} variations is well defined, it will be used as the standard value for the soliton generation period T_s. Thus $T_s = 32.4$ for the positive forcing shown in figure 1.

For the case of negative forcing shown in figure 2, it is of interest to note that (*a*) the drag has a slightly longer period than in the case of positive forcing, with $T_s = 34.8$ here; (*b*) the instantaneous drag fluctuation is skewed in phase (suggesting that it has two or more harmonics) and with a larger magnitude than in the case of positive forcing, even becoming negative within a small part of the period but it has a positive mean of $\overline{C}_{D_w} = 0.036$; and (*c*) the depressed water region behind the forcing is not as uniform in depth as in the former case, apparently owing to a succession of very small waves traversing backward across the region, recoiling from the forcing. Further, a closer examination of the numerical results shows that (*d*) the local wave continues to be excited to a relatively quite large amplitude within the region of the (negative) forcing before it breaks away, soon to settle to a smaller height after departure, as if in overcoming a threshold. These features are common to all negative forcings.

Without further detailed comparison between theory and experiment, we may summarize the findings by Lee (1985) as follows. Both the generalized Boussinesq and fKdV models are found to be in broad agreement with the experimental results for the topography mode, particularly when the speed is nearly critical ($0.9 < F < 1.1$) and when the disturbance is not excessively strong ($P_m < 0.15$). Further details can be found in Lee (1985). With the validity so established, the fKdV model therefore appears especially appropriate for the analytical development of a stability theory for forced nonlinear waves, primarily because of its simplicity.

Before we pursue this course, it is worth noting that the solutions given in figures 1 and 2 illustrate the following salient features: (i) the existence of the unperturbed uniform state both ahead of the precursor solitons and behind the trailing wavetrain; (ii) the existence of another uniform state in the region of depressed water immediately behind the disturbance; and (iii) the time-periodic generation of solitons, the typical time period being found to be large on the scale of h_0/c_0. These unique features can be utilized for carrying out mass, momentum and energy considerations based on the fKdV model to obtain a set of approximate relations between key flow quantities, as discussed by Wu (1985, 1986), and will be shown below.

4. A mass, momentum and energy theorem

We consider the nonlinear wave problem illustrated in figure 3. In the body frame, as shown in figure 3(*b*), the incident flow comes from the free-stream uniform state with water depth h_0 and velocity U. Here for simplicity we shall limit ourselves to the critical case of $U = c_0 = (gh_0)^{\frac{1}{2}}$ so that the Froude number $F = U/c_0 = 1$, since extension to small values of $|F-1|$ is straightforward. The length, time and velocity will be scaled, as before, by $h_0, h_0/c_0$ and c_0. The main features of the flow described above will be taken as given for carrying out the present mass, momentum and energy considerations. Thus the flow in the vicinity of the obstacle is not steady, but undergoes a cyclic motion, producing solitary waves to progress upstream with velocity $c_a - U$ relative to the body (or the topography), c_a being the amplitude-dependent phase velocity in the fluid frame. There are two more regions of uniform state, one being with depth h_1 and fluid velocity U_1 in the region of depressed water just behind the topography and the other being the free-stream state recovered downstream of the wavetrain. The leading wave of the trailing wavetrain and its distal end recede rearward with velocities $U - c_{g1}$ and $U - c_{g0}$, respectively, c_{g1} and c_{g0} being the pertinent (amplitude-dependent) group velocities with reference to the fluid frame. Three typical stations fixed in these three regions of uniform state are designated by $x = x_0, x_1$, and x_2, while x_L and x_T refer to the leading and trailing edges of the topography.

In the vicinity of the obstacle, new solitary waves are generated periodically, with time period T_s. Variations in wave properties are assumed sufficiently gradual (T_s large on the scale of h_0/c_0) for local and regional averages to be definable over periods of T_s. Each new solition generated, with amplitude $a(=\alpha h_0)$, contributes an excess

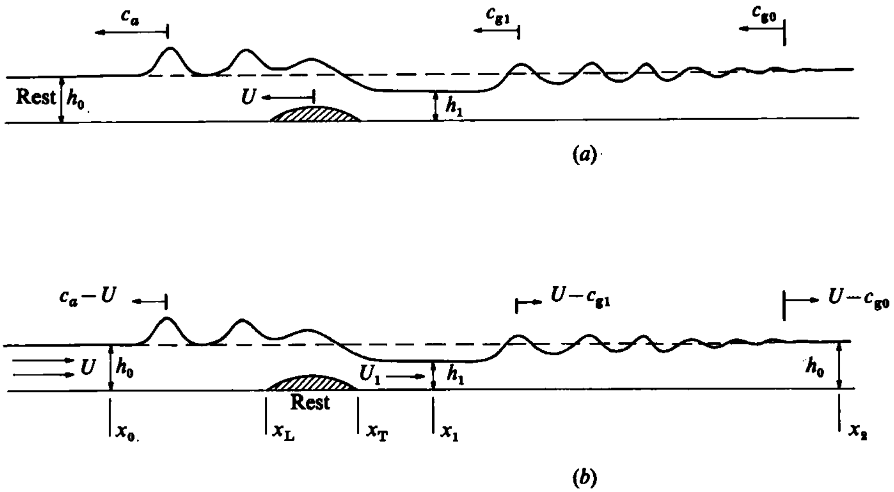

FIGURE 3. Illustration of transcritical water-wave problem: (*a*) an obstacle moving at constant transcritical velocity U in a uniform layer of water initially at rest; (*b*) obstacle fixed in a uniform stream of velocity U.

mass m_s and total energy E_s to the upstream side of the topography, where, in dimensionless form,

$$m_s = 4(\tfrac{1}{3}\alpha)^{\frac{1}{2}}, \quad E_s = 8(\tfrac{1}{3}\alpha)^{\frac{3}{2}}. \tag{25}$$

For $F = 1$, the fKdV equation (15) (in the body frame) becomes

$$\zeta_t - \tfrac{3}{2}\zeta\zeta_x - \tfrac{1}{6}\zeta_{xxx} = \frac{1}{2}\frac{\mathrm{d}}{\mathrm{d}x}P(x), \tag{26}$$

where P is given in $x_L < x < x_T$ and vanishes elsewhere. Integrating (26) from $x = x_0$ (at which $\zeta = 0$) to x_1 (at which $\zeta = h_1 - 1 < 0$), we have

$$\frac{\mathrm{d}}{\mathrm{d}t}\int_{x_0}^{x_1} \zeta \,\mathrm{d}x = \tfrac{3}{4}(1-h_1)^2,$$

which has the average

$$\frac{m_s}{T_s} = \tfrac{3}{4}(1-h_1)^2. \tag{27}$$

Here, the result $m_s/T_s \geqslant 0$ also implies, by a mass-conservation argument, that $0 < h_1 \leqslant 1$. Integrating (26) from $x = x_0$ to the leading edge of the topography at x_L gives

$$\frac{\mathrm{d}}{\mathrm{d}t}\int_{x_0}^{x_L} \zeta \,\mathrm{d}x = \tfrac{3}{4}\zeta_L^2 + \tfrac{1}{6}\zeta_{Lxx},$$

where $\zeta_L(t) = \zeta(x_L, t)$, with the compositions $\zeta_L = \bar{\zeta}_L + \zeta_L'(t)$, $\bar{\zeta}_L$ being the average of $\zeta_L(t)$. The oscillatory component ζ_L' will be assumed small in amplitude (compared with $|\bar{\zeta}_L|$) on the physical grounds that a mean slope of the water surface is needed to provide the rate of work by P required for overcoming the wave resistance, and ζ_L' relatively is a slow and weak modulation. We shall take the case of positive forcing (or vice versa for negative forcing) where there is an extra horizontal pressure gradient from the trailing to the leading edge of the forcing distribution, rendering $\bar{\zeta}_L$ greater than $\bar{\zeta}_T$, the mean elevation at the trailing edge. We further assume that ζ has a negligible curvature as expected of long waves. Then the above equation has the average

$$\frac{m_s}{T_s} = \tfrac{3}{4}(\bar{\zeta}_L)^2. \tag{28}$$

Hence, by (27) and (28),

$$\bar{\zeta}_L = 1-h_1. \tag{29}$$

For the energy consideration, we integrate the product of (26) with ζ from $x = x_0$ to x_1, giving

$$\frac{d}{dt}\int_{x_0}^{x_1} \tfrac{1}{2}\zeta^2\,dx = \tfrac{1}{2}(C_{D_w}+\zeta^3(x_1)),$$

which has the average

$$\frac{E_s}{T_s} = \bar{C}_{D_w}-(1-h_1)^3. \tag{30}$$

A separate account for the energy conservation between $x = x_0$ and the leading edge x_L yields, under the same assumption as that invoked in attaining (28), the relation

$$\frac{E_s}{T_s} = \bar{\zeta}_L^3 = (1-h_1)^3. \tag{31}$$

Next, the ratio of E_s/m_s derived from (25), (27) and (31) gives

$$\frac{E_s}{m_s} = \tfrac{2}{3}\alpha = \tfrac{4}{3}(1-h_1), \tag{32}$$

whence

$$\alpha = 2(1-h_1). \tag{33}$$

The period of generation T_s can now be expressed, by using (25) and (27) or (31), in terms of a single parameter as

$$T_s = \frac{64}{(3\alpha)^{\frac{3}{2}}} = \frac{12.3}{\alpha^{\frac{3}{2}}}. \tag{34}$$

The mean drag coefficient can be deduced from (30)–(34) as

$$\bar{C}_{D_w} = \tfrac{1}{4}\alpha^3. \tag{35}$$

The cnoidal-like wavetrain trailing the region of a nearly uniform flow (with a depressed surface) behind the forcing, which may seem at first glance to resemble an undular bore, has some refined features of its own. Classical bores and undular bores usually describe a transition between an incoming uniform stream and an ensuing one, generally pertaining to steady transitions of a closed hydromechanical system with internal dissipation. Benjamin & Lighthill (1954) showed that steady inviscid bores, or broadly the transitions from a uniform stream to a uniform wavetrain with the same values of volume flow rate, specific flow energy (per unit mass) and specific flow force (the total momentum flux) (Q, R, S in the original notation) are impossible. Thus, a uniform train of cnoidal waves cannot form an undular bore. With time and space variations allowed, the development of inviscid bores from initial states has been investigated by Peregrine (1966) for continuous distributions and by Fornberg & Whitham (1978) for steps and well forms. These studies still pertain to closed systems.

A new feature of the unsteady trailing wavetrain in the present case is that both the amplitude and length of the wavetrain grow with a continuous intake of energy from the forcing disturbance, thus signifying a system open to external excitation.

To determine this energy supply, a simple approach is to integrate the energy equations of (26) from $x = x_1$ to $x = x_2$, with the result

$$\frac{\mathrm{d}}{\mathrm{d}t}\int_{x_1}^{x_2} \zeta^2\,\mathrm{d}x = (1-h_1)^3.$$

The time average of this equation gives

$$\frac{\mathrm{d}E_{\mathrm{Tw}}}{\mathrm{d}t} = (1-h_1)^3 = (\tfrac{1}{2}\alpha)^3, \tag{36}$$

where E_{Tw} represents the energy that the trailing wavetrain receives from the forcing disturbance. This rate of increase in wave energy implies that the forcing agent must overcome a resistance, in coefficient form, of the value

$$C_{D_\mathrm{s}} = (\tfrac{1}{2}\alpha)^3 = \tfrac{1}{2}\overline{C}_{D_\mathrm{w}}, \tag{37}$$

which is a component of the total wave resistance C_{D_w}. Unlike the wave-resistance component pertaining to the generation of upstream-advancing solitons, which is time periodic, the component C_{D_s} associated with the trailing wavetrain soon becomes steady, after shedding distally the first few waves.

In addition, we can obtain a few more relationships of kinematical interest. From the continuity relation between stations x_0 and x_1, $Uh_0 - U_1 h_1 = m_\mathrm{s}/T_\mathrm{s}$, we obtain for the Froude number $F_{10} = U_1/c_0$ of the depressed flow behind the topography the result

$$F_{10} = \frac{1}{h_1}[1-\tfrac{3}{4}(1-h_1)^2]. \tag{38}$$

For the motion of the trailing wavetrain, let the zero-crossing ($\zeta = 0$) of the leading wave in the train move backward with velocity $U_{0\mathrm{c}}$ relative to the obstacle. By considering mass and momentum conservation in the frame fixed to the trailing wave, one can find that

$$F_{0\mathrm{c}} = \frac{U_{0\mathrm{c}}}{c_0} = 1-[\tfrac{1}{2}h_1(1+h_1)]^{\frac{1}{2}}. \tag{39}$$

From the above we immediately see that provided $\overline{C}_{D_\mathrm{w}} \geqslant 0$ (for otherwise we would have had a perpetual machine), we have $\alpha \geqslant 0$ by (35), $0 \leqslant h_1 \leqslant 1$ by (33), and $F_{10} \geqslant 1$ (supercritical) and $F_{0\mathrm{c}} \leqslant 1$ (subcritical) by (38) and (39).

Finally, we note that the relationships between key flow quantities given by the present first-principle theorem, falling short of producing the detailed solution like all momentum theorems, still depend on two flow parameters, namely, the Froude number F (which is a free parameter, equal to 1 here) and any one of the other quantities involved (whose value may be empirically furnished), e.g. the mean wave-resistance coefficient $\overline{C}_{D_\mathrm{w}}$, to which there can correspond different forcing distributions.

For a comparison between the present approximate predictions and numerical results, calculations were performed for the cosine forcing distribution (18) with

$$F = 1, \quad P_\mathrm{m} = 0.1, \quad h_0 = 1, \quad L = 2. \tag{40}$$

The main numerical results are presented in figure 4; they provide the following data given in table 1 for comparison with the approximate predictions based on the same value of h_1. The approximate predictions are in good agreement with the numerical results and well represent other cases not shown.

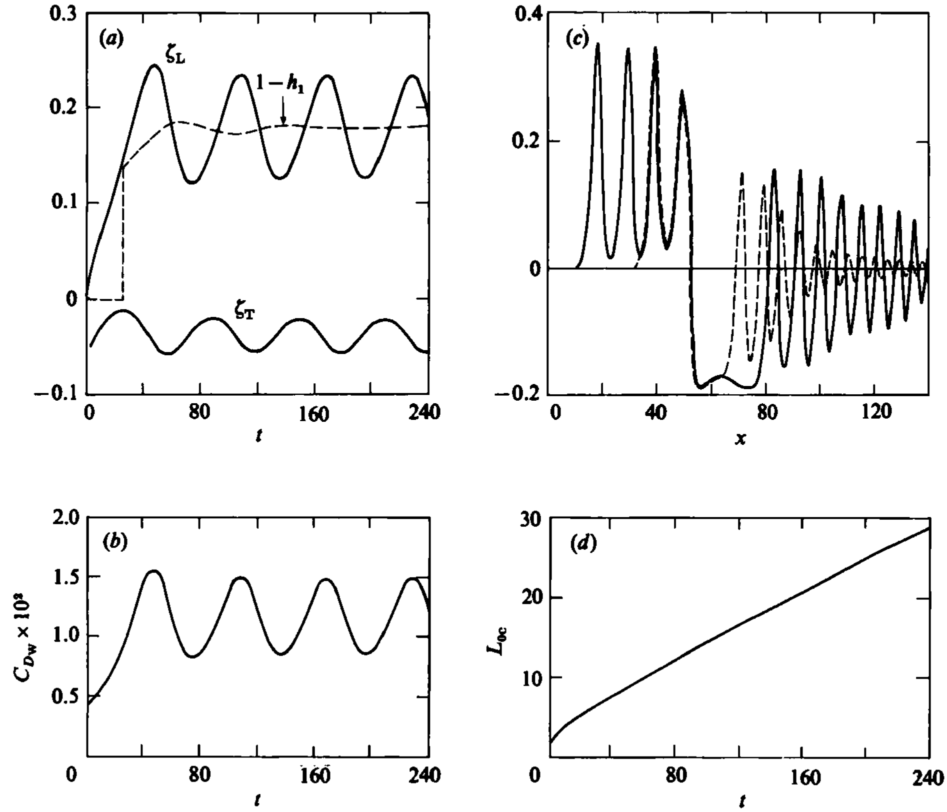

FIGURE 4. Numerical results of the fKdV model for some pertinent flow quantities generated by the cosine forcing function (18) with $P_m = 0.1$ at Froude number $F = 1$: (a) $1-h_1$, ζ_L, ζ_T (the wave elevation at x_1, x_L and x_T); (b) wave resistance coefficient C_{D_w}; (c) wave profiles at $t = 60$ (— — —), and at $t = 120$ (——); (d) L_{0c} is the distance between the trailing edge x_T and the zero-crossing of the first trailing wave. (Here the leading and trailing edges of the topography are at $x_L = 50$ and $x_T = 52$.)

Equation	Approximate prediction	Numerical result
base	$1-h_1 = 0.18$	$1-h_1 = 0.18$
(33)	$\alpha = 0.36$	$\alpha = 0.355$
(29)	$\overline{\zeta}_L = 0.18$	$\overline{\zeta}_L = 0.18$
(34)	$T_s = 57$	$T_s = 58$
(35)	$\overline{C}_{D_w} = 0.012$	$\overline{C}_{D_w} = 0.013$
(38)	$F_{10} = 1.19$	$F_{10} = 1.20$
(39)	$F_{0c} = 0.8$	$F_{0c} = 0.89$

TABLE 1. Comparison between numerical results and an approximate prediction

In concluding this comparative study, we remark that the present theorem does not preclude the particular class of transcritical forcing functions that can maintain the fluid response being locally confined and permanently stationary. Such forced steady solitary waves do exist and they must necessarily have zero drag coefficient, $C_{D_w} = 0$, for then $\alpha = 0$ by (35), $h_1 = 1$ by (33), implying that no upstream-advancing solitons will be generated. This important particular class will be investigated below.

5. Forced steady solitary waves

It is of basic interest to find exact solutions of the fKdV equation (15) that belong to the class of forced solitary waves of permanent form when coupled with appropriate steadily moving forcing functions. These solutions can play several significant roles. First, they may be used to gauge the uniform validity of any approximate method used for the fKdV model. Moreover, they can provide an initial basis for developing nonlinear stability theory for the fKdV class of flows.

A forced permanent solitary wave is required to satisfy the equation

$$(F-1)\zeta-\tfrac{3}{4}\zeta^2-\tfrac{1}{6}\zeta_{xx}=\tfrac{1}{2}P(x), \tag{41}$$

which is the first integral of (15) obtained with $\zeta_t=0$, and to satisfy the regularity conditions that ζ and P vanish at $x=\pm\infty$. Here $P(x)=p_{\mathrm{a}}(x)+b(x)$ represents in totality the disturbances p_{a} and b. Equation (41) has the following time-independent solutions, which decay exponentially at infinity for a given N ($N=1,2,\ldots$):

$$\zeta_{\mathrm{s}}=\sum_{n=1}^{N} a_n \operatorname{sech}^{2n} kx, \tag{42}$$

$$P=2\sum_{n=1}^{2N} b_n \operatorname{sech}^{2n} kx, \tag{43a}$$

$$b_n=F_n a_n+k^2B_n a_{n-1}-\frac{3}{4}\sum_{m=1}^{n-1} a_m a_{n-m} \quad (n=1,2,\ldots,N+1), \tag{43b}$$

$$b_n=-\frac{3}{4}\sum_{m=n-N}^{N} a_m a_{n-m} \quad (n=N+2,\ldots,2N), \tag{43c}$$

$$F_n=(F-1)-\tfrac{2}{3}k^2n^2, \tag{43d}$$

$$B_n=\tfrac{1}{3}(n-1)(2n-1), \tag{43e}$$

where the a_n are real constants, $a_n=0$ for $n<1$ and $n>N$ being understood. Equations (43*b*–*e*) are $2N$ relations between $(b_1,\ldots,b_{2N})$ and $(a_1,\ldots,a_N)$. It is therefore clear that in general, $(b_1,\ldots,b_{2N})$ and hence $P(x)$ cannot be arbitrarily prescribed since in the physically direct, mathematically inverse prescription with the b_n arbitrarily given, there may be no real solution for all the a_n. But one can always take the mathematically direct, physically inverse approach by regarding $(a_1,\ldots,a_N)$ as generalized coordinates for prescribing ζ, and hence have P uniquely determined by (43). Following the latter approach, we then see that by a uniqueness argument (see the Appendix), the solutions given by (42) and (43) are unique, stationary solutions of the fKdV equation (15) provided they further satisfy the initial condition

$$\zeta(x,0)=\zeta_{\mathrm{s}}(x) \quad (-\infty<x<\infty). \tag{44}$$

Thus, (42)–(44) constitute a family of an infinity of time-independent solutions of the fKdV equation (15). All these forced steady solitary waves are localized (falling off exponentially at large distances) and are symmetric with respect to $x=0$. However, aside from accompanying the solitary wave by moving steadily at some feasible Froude number F (which can be rather arbitrarily assigned, even to subcritical values in some cases), the forcing function $P(x)$ does no mechanical work. In fact, the symmetry of ζ_{s} and P (both being even in x) implies that the wave-resistance integral in (23) vanishes,

$$D_{\mathrm{w}}=0. \tag{45}$$

The same result is obtained upon integration of the wave-resistance integral using (41). This is expected on physical grounds since when (44) is also satisfied, the steadily moving wave has no initial excess energy to radiate off the forcing region, and this implies that the excess energy will remain zero.

For given N, the solution is characterized by $(F, k, a_1, \ldots, a_N)$ as $N+2$ parameters. One of the simplest members of this family of solutions is the one-term forced soliton

$$\zeta_{s1} = a \operatorname{sech}^2 kx, \tag{46a}$$

with

$$b_1 = F_1 a, \quad b_2 = a(k^2 - \tfrac{3}{4}a), \quad b_3 = b_4 = \ldots = 0. \tag{46b}$$

Here the subscript of a_1 has been omitted for brevity. Three special cases are of particular interest:

(I) One-term forcing function I: the choice of $b_1 \neq 0$ and $b_2 = 0$ gives

$$\zeta_{s1} = a \operatorname{sech}^2 kx, \quad a = \tfrac{4}{3}k^2, \tag{47a}$$

$$P_{11} = 2b_1 \operatorname{sech}^2 kx, \tag{47b}$$

$$b_1 = F_1 a, \quad F_1 = (F-1) - \tfrac{2}{3}k^2. \tag{47c}$$

(II) One-term forcing function II: the choice of $F_1 = 0$ and $a \neq 0$ gives

$$\zeta_{s1} = a \operatorname{sech}^2 kx, \tag{48a}$$

$$P_{12} = 2b_2 \operatorname{sech}^4 kx, \tag{48b}$$

$$F_1 = F - 1 - \tfrac{2}{3}k^2 = 0, \quad b_2 = a(k^2 - \tfrac{3}{4}a), \tag{48c}$$

which is the solution obtained by Patoine & Warn (1982).

(III) Vanishing forcing function: the choice of $a \neq 0$, $F_1 = 0$ and $b_2 = 0$ gives

$$\zeta_{s1} = a \operatorname{sech}^2 kx, \quad a = \tfrac{4}{3}k^2, \tag{49a}$$

$$F = F_0 \equiv 1 + \tfrac{1}{2}a, \tag{49b}$$

$$P = 0, \tag{49c}$$

which is the familiar free-soliton solution and is the limiting case of the previous two families of forced solitons as the forcing functions P_{11} and P_{12} tend to zero. We note that for type I forcing, (47c) shows that F_1, and hence the Froude number F can be chosen rather arbitrarily, and can even be subcritical. Here in case (I), ζ_{s1} is always a positive wave and the forcing function P_{11} is positive or negative according as F is $>$ or $<$ $F_0 \equiv 1 + \tfrac{1}{2}a$, respectively. For type II forcing, however, F can only be supercritical and it is necessary that $b_2 < \tfrac{4}{3}k^4$ to render a real. We further note that the class I forced soliton (47a) and free soliton (49a) have the same shape function, but they generally have different phase velocities.

Finally, we remark that the initial condition (44) seems sufficient to ensure that a forced steady solitary wave, if once established, will remain permanent in shape as long as it is accompanied by the congruent forcing function. However, it is not known whether, if (44) is not satisfied, by whatever the margin, there will always be a finite difference between the resulting motion (satisfying the fKdV equation) and the stationary solution for the same forcing function. This possibility naturally leads to the question of the stability of forced steady solitary waves.

6. A perturbation theory for soliton generation

Suppose a forced steady soliton solution $\zeta_s(x)$ of (41) is given an arbitrary (but sufficiently smooth) initial perturbation $\eta_0(x)$, which we shall regard as the initial value of a 'perturbation function' $\eta(x,t)$. The problem of primary interest is to determine the stability of the resultant motion:

$$\zeta(x,t) = \zeta_s(x) + \eta(x,t), \tag{50}$$

which is required to satisfy the fKdV equation (15). Substituting (50) into (15) and noting that $\zeta_s(x)$ satisfies (41), we obtain for η the following homogeneous evolution equation:

$$\eta_t + \frac{\partial}{\partial x}[(F-1)\,\eta - \tfrac{3}{4}\eta^2 - \tfrac{1}{6}\eta_{xx} - \tfrac{3}{2}\zeta_s\eta] = 0. \tag{51}$$

The problem then becomes one of calculating η from (51) under the initial condition

$$\eta(x,0) = \eta_0(x) \quad (-\infty < x < \infty). \tag{52}$$

A closely related problem is to study the linear stability of the perturbation $\eta(x,t)$ which is governed by the linearized equation of (51),

$$\eta_t + \frac{\partial}{\partial x}[(F-1)\,\eta - \tfrac{1}{6}\eta_{xx} - \tfrac{3}{2}\zeta_s\,\eta] = 0. \tag{53}$$

By separation of variables, $\qquad \eta(x,t) = \mathrm{e}^{\sigma t} f(x), \qquad (54)$

the linear stability analysis reduces to the calculation of the eigenvalues σ of the ordinary differential equation

$$\frac{\mathrm{d}}{\mathrm{d}x}[(F-1)f - \tfrac{1}{6}f_{xx} - \tfrac{3}{2}\zeta_s f] + \sigma f = 0, \tag{55}$$

for $-\infty < x < \infty$, with the solution vanishing at $x = \pm\infty$. This eigenvalue problem does not seem to have been resolved.

Let us take recourse to numerical experiments using the original nonlinear equation (51) and take for ζ_s the simple solution ζ_{s1} given by (47). With this choice of ζ_{s1}, we note that by applying the following similarity transformation:

$$\eta = k^2\eta', \quad x' = kx, \quad t' = k^3 t, \quad F-1 = k^2(F'-1), \tag{56}$$

(51) becomes $\qquad \dfrac{\partial\eta}{\partial t} + \dfrac{\partial}{\partial x}[(F'-1)\,\eta - \tfrac{3}{4}\eta^2 - \tfrac{1}{6}\eta_{xx} - \tfrac{3}{2}\zeta'_s\,\eta] = 0, \qquad (57a)$

where the primes have been omitted for η', x' and t' (but not for F' and ζ'_s for ease of identification, and the prime may be restored when needed) and

$$\zeta'_s = \tfrac{4}{3}\,\mathrm{sech}^2\, x. \tag{57b}$$

Thus we see that all the k have cancelled out in (57a, b) and hence the solution η (or rather η') will not depend on k if the initial condition

$$\eta(x,0) = \eta_0(x) \tag{57c}$$

is also independent of k. After the parameter k is so eliminated, the computation seems to be greatly simplified to one for the universal case prescribed by (57a–c) in which only one parameter, namely F', remains. However, it is essential to recall that in order to avoid certain ill-conditioned numerical instabilities, it is necessary to

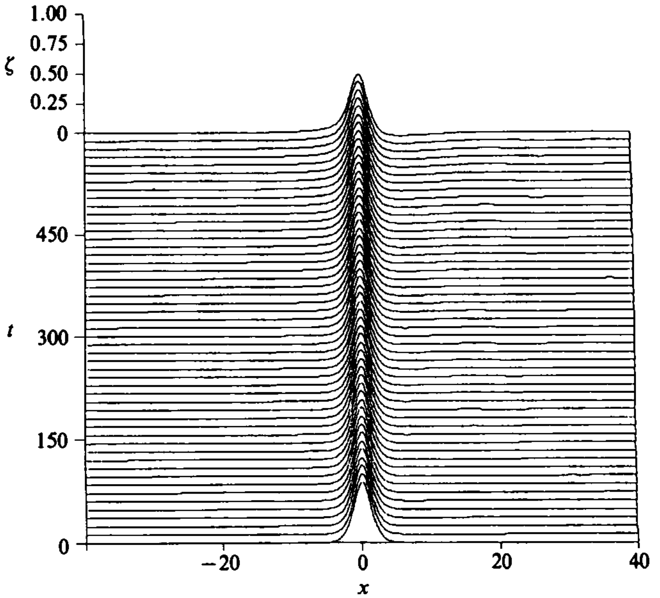

FIGURE 5. Numerical results of the fKdV model exhibiting the very high degree of stability of the forced steady solitary wave (47 *a–c*) when initially so established, moving at $F = 1$ under stationary forcing $P = 2b_1 \operatorname{sech}^2 kx$, with $k = 0.6124$ ($a = 0.5$) and amplitude $P_m = 2b_1 = -0.25$, over the duration $0 < t < 600$ (with a relative error less than 2% after having traversed over a distance of 600 water depths). Calculation was made with $\Delta x = 0.05$ and $t = 0.025$).

employ not the original but the regularized fKdV equation, which reads in the body frame (moving to the left with velocity $U = c_0 F$), in dimensionless form, as

$$\zeta_t + (F - 1 - \tfrac{3}{2}\zeta)\,\zeta_x - \tfrac{1}{6}[\zeta_{xxt} + F\zeta_{xxx}] = \tfrac{1}{2}P_x. \tag{58}$$

For given P and initial condition, the solution ζ of (58) has, with respect to the solution of the original fKdV equation (15), an error factor $[1 + O(|\zeta|)]$, which is $[1 + O(k^2\alpha)]$ in terms of the similarity variables defined in (56). Thus, the smaller the value of k, the more accurately the regularized fKdV equation can approximate the original fKdV equation, or equivalently (57). On the other hand, the smaller the value of k, the larger the number of time-steps that will be required for computation according to the similarity relation. Therefore, an optimum choice of the range of k-values was made for the computation as desired.

Keeping this in mind, we have carried out two series of calculations to numerically investigate the stability of η. In the first, the initial value of ζ assumes the forced steady solution without any perturbation,

$$\zeta(x, 0) = \zeta_s(x), \quad \text{or} \quad \eta(x, 0) = \eta_0(x) \equiv 0. \tag{59}$$

The results of all the cases computed under condition (59) show that the initial stationary solution remained virtually permanent in form while being accompanied by the steady forcing. As exemplified in figure 5 for the critical case of $F = 1$, with $k = 0.6124$ ($a = 0.5$) and forcing amplitude $P_m = 2b_1 = -0.25$, the forced steady solitary wave, when so established initially, remained globally stable over the duration $0 < t < 600$ for which computation was executed, with only a relative error less than 2% after the wave had traversed the distance of 600 water depths. As this relative error is consistent with those for *free* solitary waves computed by the present

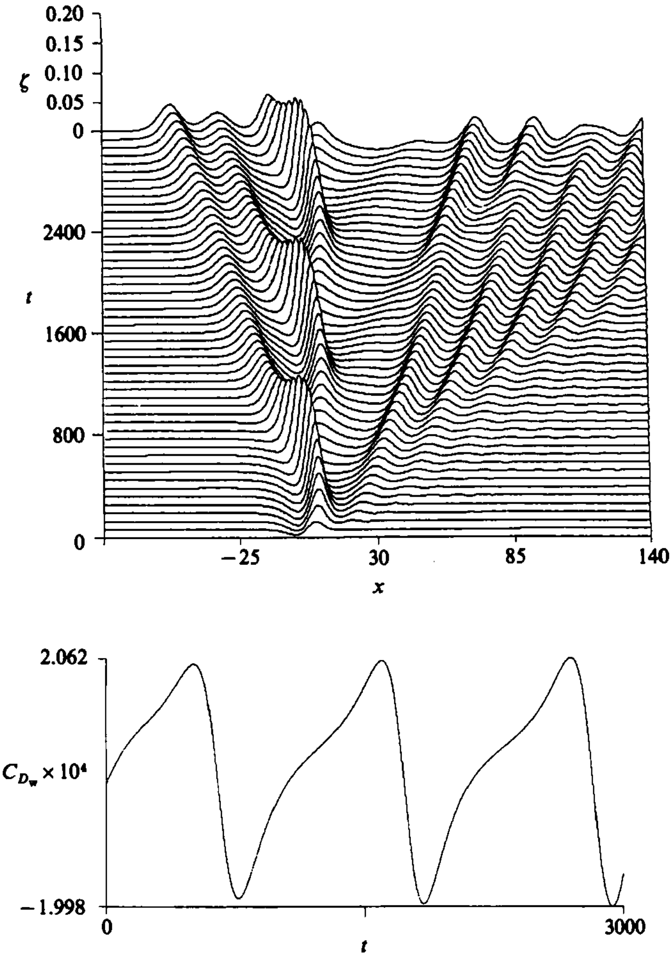

FIGURE 6. Numerical results of the fKdV model showing the evolution of waves generated from the initial state of rest by stationary forcing (47*b*) at $F = 1$, with $k = 0.1936\,(a = 0.05)$ and amplitude $P_m = -0.0025$. The wave-resistance coefficient varies with period $T_s = 1{,}090$.

numerical method, the result may thus be regarded as signifying that small numerical perturbations (which would be inevitable) remained small throughout the computation. However, this result does not necessarily imply stability of the forced steady-state solution.

In the second series of calculations, the rest state of ζ was assigned as the initial value, namely,

$$\zeta(x,0) = 0, \quad \text{or} \quad \eta_0(x) = \eta(x,0) = -\zeta_s(x). \tag{60}$$

This initial deviation from the steady-state solution is but one of infinitely many possible choices as a perturbation of the stationary solution. Nevertheless, it is the most convenient of all choices for making comparisons with experiments, both existing and new, as well as with those forcing functions that do not possess stationary solutions. By using the regularized version of (15) and the numerical code specially developed for this purpose, results have been obtained for the generation and evolution of forced long waves for the critical case of $F = 1$, with some of the results

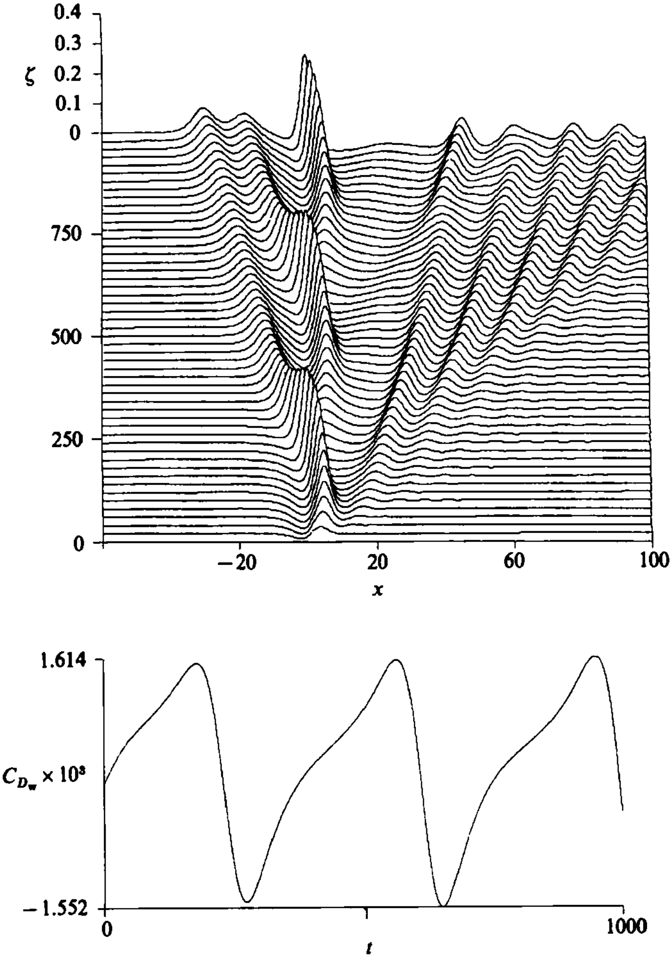

FIGURE 7. The fKdV-model results for waves generated from the initial rest state by stationary forcing (47*b*) at $F = 1$, with $k = 0.2739\,(a = 0.10)$ and amplitude $P_m = -0.01$. The wave resistance varies with period $T_s = 387$.

presented graphically in figures 6–8 over a range of the parameters involved and with some pertinent flow quantities listed in table 2. In the cases computed under condition (60), new waves are invariably found to evolve from the initial disturbance given by (60), leading in time to the process of periodic generation of upstream-advancing solitary waves, with a definite period in each case, and with the mean height of the first three precursor solitons denoted by α. On the downstream side, they are followed by a lengthening region of depressed water, and further behind by a lengthening train of cnoidal-like waves. The main features of the wave system developed by this family of forcing are thus very similar to those found earlier for the moving cosine-shaped topography as shown in figures 1 and 2.

To obtain the universal constant value for T'_s (the period of soliton generation) for the system (57*a*, *b*) and (60) (in the similarity form), we exploit the numerical results for T_s determined from the regularized fKdV equation as given in table 2, which by extrapolation to $k = 0$ yields

$$T'_s = 7.9(\pm 0.04). \tag{61}$$

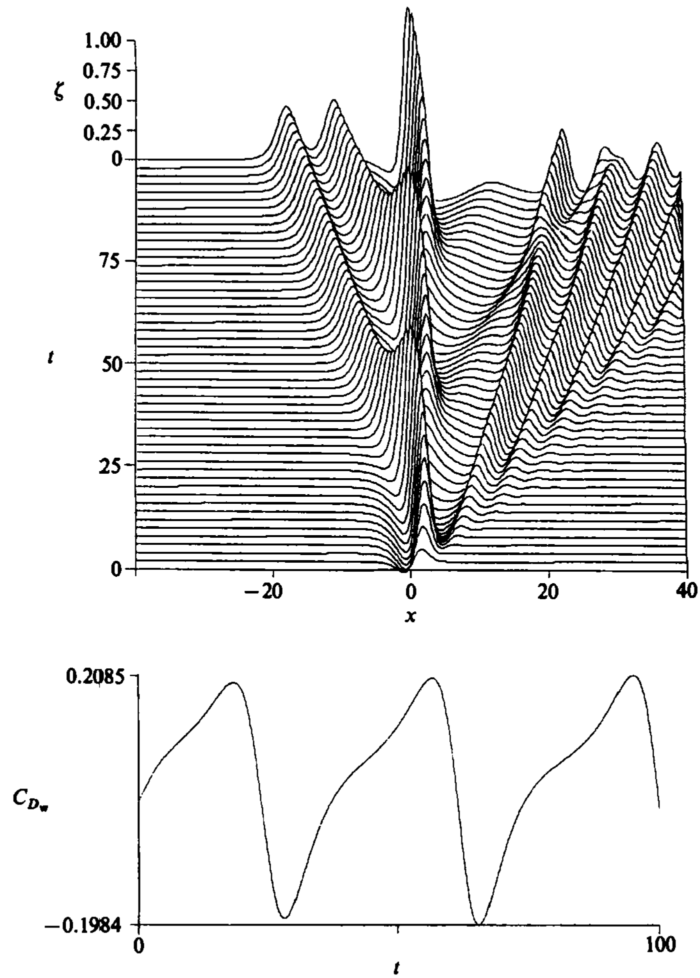

FIGURE 8. The fKdV-model results for waves generated from the initial rest state by stationary forcing (47*b*) at $F = 1$, with $k = 0.6124$ ($a = 0.50$) and amplitude $P_m = -0.25$. The wave resistance varies with period $T_s = 38$.

a	k	$P_m = 2b_1$	T_s	$T_s' = T_s k^3$	$\Delta C_D/k^6$	α
0.05	0.1936	−0.0025	1,090	7.91	7.71	0.045
0.10	0.2739	−0.01	387	7.94	7.50	0.092
0.50	0.6124	−0.25	38	8.6	7.65	0.50

TABLE 2. Flow quantities

Restoring the original variable by (56), we therefore have

$$T_s = \frac{7.9}{k^3}, \tag{62}$$

or in terms of the amplitude $a(=\frac{4}{3}k^2)$ of the forced steady soliton

$$T_s = \frac{11.5}{a^{\frac{3}{2}}}, \tag{63}$$

or based on the amplitude $P_m(=-a^2)$ of the forcing function,

$$T_s = \frac{11.5}{|P_m|^{\frac{3}{4}}}. \tag{64}$$

These are the various similarity relations for the period of soliton generation for this one-parameter family under the initial condition (60) for the critical case of $F = 1$.

It is of interest to compare the above solution for T_s with the approximate formula (34) obtained by mass, momentum and energy considerations:

$$T_s = \frac{12.3}{\alpha^{\frac{3}{2}}}.$$

The two formulas (63) and (34) are very similar in form; they in fact can be further reconciled. Although a and α are different by definition (a being the amplitude of a forced steady soliton and α the amplitude of a free solitary wave), they are found here (for the case of $F = 1$) to be nearly equal (within a 10% difference) as shown in table 2, where the α-value represents the numerical mean height of the first three precursor solitons. This may be expected on the physical grounds that precursor solitons occur only in the resonant state of the system and evolve on the slow timescale, so the forced and free solitons should have about the same k and hence, by (47a) and (49a), are nearly equal in height. However, we should notice the functional differences between the two forcing distributions (18) and (47). Moreover, if the amplitude P_m of a forcing function, like (18), does not scale like the b_1 in (47) (which scales by (56) with a factor of k^4 or α^2), the T_s formula should then have a new factor,

$$T_s = \frac{1}{\alpha^{\frac{3}{2}}} H\left(\frac{P_m}{\alpha^2}\right), \tag{65}$$

with $H(P_m/\alpha^2)$ providing the correction to the off-scale of the obstacle height. The present results seem to suggest that T_s may only be mildly sensitive to variations of the strength and shape of the forcing function if the wave resistance is held equal as a reference parameter, as conjectured at the end of §3.

In addition, we have listed in table 2 numerical results for $(\Delta C_D)/k^6$, where ΔC_D is the difference between the maxima and minima of C_{D_w}. The nearly constant value of this quantity over the broad range of k is in accord with the similarity relation (35).

In conclusion, we shall summarize the numerical results for the cases characterized by the initial perturbations (59) and (60). In the first case with infinitesimal initial perturbations (such small perturbations would be inevitable in a numerical calculation), the forced steady solitons are found to remain stable over time periods of computation many times the period of T_s given by (62). This is consistent with the uniqueness theorem of the Appendix, according to which an initially established forced steady solution, if stable, will remain permanent in form. In contrast, in the second case when the steady solution is impulsively imposed on the initial state of rest, new solitons are found to be generated with the period of T_s. In view of these drastically different results, it seems that the study of the underlying mechanism could be further illuminated by introducing a new parameter μ such that the initial condition now assumes the form

$$\eta(x,0) = -\mu\zeta_s(x), \quad \text{or} \quad \zeta(x,0) = (1-\mu)\,\zeta_s(x). \tag{66}$$

This condition becomes (59), the first case with zero initial perturbation, when $\mu = 0$, and becomes (60), the second case with the initial state of rest, when $\mu = 1$. The critical point separating the regions of occurrence and non-existence of precursor solitons would therefore lie in the range $0 < \mu < 1$. The new problem will thus be that of finding if there exists a certain positive constant $\mu_c, 0 < \mu_c < 1$, such that the forced steady solution undergoes a time periodic bifurcation for $\mu > \mu_c$ and otherwise for $0 \leqslant \mu < \mu_c$. Study in this direction is continuing to determine the basic mechanism underlying the phenomenon.

This work was jointly sponsored by ONR Contract N00014-85-K-0536, NR655-005 and NSF Grant MSM-8118429, A03, and was presented at the Symposium on *Fluid Mechanics in the Spirit of G. I. Taylor* held in Cambridge in March 1986. The paper was submitted to the *Journal of Fluid Mechanics* for publication in the special Symposium volume (number 173, December 1986), but being delayed by the need for revision was not ready in time for publication in that volume. I am grateful to the referees for a number of enlightening comments and for pointing out a few publications of geophysical context. I am also indebted to George Yates and Jinlin Zhu for helpful discussions and for their valuable assistance in obtaining the numerical results presented here. The numerical calculations were done on the CRAY-1 at the Naval Research Laboratory (sponsored by the Office of Naval Research) and on the CRAY X-MP/48 at San Diego Supercomputer Center (operated by the National Science Foundation).

Appendix. A uniqueness theorem for the forced KdV model

We consider C^N solutions of (15), defined for sufficiently large positive integer N and for all x in $(-\infty, \infty)$, with ζ and all its x-derivatives tending to zero as $x \rightarrow \pm\infty$, and with the forcing functions satisfying similar conditions (namely, being of the C^{N-2} class). It can then be shown that such solutions are uniquely determined by their forcing functions and their initial values.

Let η be another solution of (15):

$$\eta_t + (F-1-\tfrac{3}{2}\eta)\,\eta_x - \tfrac{1}{6}\eta_{xxx} = \tfrac{1}{2}(p_a+b)_x, \tag{A 1}$$

and let both ζ and η satisfy the same initial condition. The difference between (15) and (A 1) yields for $w = \zeta - \eta$ the linear equation

$$w_t + (F-1)\,w_x - \tfrac{3}{2}(\zeta w_x + \eta_x w) - \tfrac{1}{6}w_{xxx} = 0, \tag{A 2}$$

and the homogeneous initial condition

$$w(x,0) = 0. \tag{A 3}$$

Multiplying (A 2) by w and integrating the result with respect to x over $(-\infty, \infty)$, we obtain, after some partial integrations, the relation

$$\frac{\mathrm{d}}{\mathrm{d}t}\int \tfrac{1}{2}w^2\,\mathrm{d}x = \frac{3}{2}\int (\eta_x - \tfrac{1}{2}\zeta_x)\,w^2\,\mathrm{d}x, \tag{A 4}$$

where we have used the fact that ζ, η and their derivatives tend to zero as $x \rightarrow \pm\infty$. From this it readily follows that

$$\frac{\mathrm{d}}{\mathrm{d}t}E(t) \leqslant KE(t),$$

where $E(t)$ is the x-integral of $\frac{1}{2}w^2$ over $(-\infty, \infty)$ and K stands for the maximum of $3|\eta_x - \frac{1}{2}\zeta_x|$. We therefore have the inequality

$$E(t) \leqslant E(0)\, e^{Kt}. \tag{A 5}$$

from which it follows that $E(t) = 0$ for all t if $E(0) = 0$, which is assured by (A 3), and hence that $w(x, t) \equiv 0$ for all x and t.

REFERENCES

AKYLAS, T. R. 1984 *J. Fluid Mech.* **141**, 455–466.

BAINES, P. G. 1977 *J. Fluid Mech.* **82**, 147–159.

BAINES, P. G. 1984 *J. Fluid Mech.* **146**, 127–167.

BENJAMIN, T. B., BONA, J. L. & MAHONY, J. J. 1972 *Phil. Trans. R. Soc. Lond.* A **272**, 47–78.

BENJAMIN, T. B. & LIGHTHILL, M. J. 1954 *Proc. R. Soc. Lond.* A **224**, 448–460.

BINNIE, A. M. & ORKNEY, J. C. 1955 *Proc. R. Soc. Lond.* A **230**, 237–246.

CHU, C. K., XIANG, L. W. & BARANSKY, Y. 1983 *Communs Pure Appl. Maths* **36**, 495–504.

COLE, S. L. 1985 *Wave Motion* **7**, 579–587.

DODD, R. K., EILBECK, J. C., GIBBON, J. D. & MORRIS, H. S. 1982 *Solitons and Nonlinear Wave Equations*. Academic.

ERTEKIN, R. C. 1984 Soliton generation by moving disturbances in shallow water: Theory computation and experiments. Ph.D. thesis, University of California, Berkeley.

ERTEKIN, R. C., WEBSTER, W. C. & WEHAUSEN, J. V. 1985 In *Proc. 15th Symp. on Naval Hydrodynamics*, pp. 347–364. Washington D.C.: National Academy Press.

ERTEKIN, R. C., WEBSTER, W. C. & WEHAUSEN, J. V. 1986 *J. Fluid Mech.* **169**, 275–292.

FAVRE, H. 1935 *Ondes de Translation*. Paris: Dunod.

FORNBERG, B. & WHITHAM, G. B. 1978 *Phil. Trans. R. Soc. Lond.* A **289**, 373–402.

GARDNER, C. S., GREENE, J. M., KRUSKAL, M. D. & MIURA, R. 1967 *Phys. Rev. Lett.* **19**, 1095–1097.

GRIMSHAW, R. H. J. & SMYTH, N. F. 1986 *J. Fluid Mech.* **169**, 429–464.

HUANG, D. D., SIBUL, O. J., WEBSTER, W. C., WEHAUSEN, J. V., WU, D. M. & WU, T. Y. 1982 In *Proc. Conf. on Behavior of Ships in Restricted Waters*, vol. II, pp. 26-1 to 26-10. Varna: Bulgarian Ship Hydrodynamics Centre.

KATSIS, C. & AKYLAS, T. R. 1987 *Phy. Fluids* **30**, 297–301.

KELLER, J. B. 1985 *Phil. Trans. R. Soc. Lond.* A **315**, 367–377.

LAX, P. D. 1968 *Communs Pure Appl. Maths* **21**, 467–490.

LEE, S. J. 1985 Generation of long water waves by moving disturbances. Ph.D. thesis, California Institute of Technology, Pasadena, CA.

MALANOTTE-ROZZOLI, P. 1984 *J. Phys. Oceanogr.* **14**, 1032–1046.

MEI, C. C. 1986 *J. Fluid Mech.* **162**, 53–67.

MILES, J. W. 1980 *Ann. Rev. Fluid Mech.* **12**, 11–43.

PATOINE, A. & WARN, T. 1982 *J. Atmos. Sci.* **39**, 1018–1025.

PEREGRINE, D. H. 1966 *J. Fluid Mech.* **25**, 321–330.

SMYTH, N. F. 1986 Modulation theory solution for resonant flow over topography. *Department of Math. Rep.* 3. University of Melbourne, Victoria, Australia.

SUN, M.-G. 1985 The evolution of waves created by a ship in a shallow canal. In *The 60th Anniv. Volume-Zhongshan University, Mechanics Essays* (in Chinese), pp. 17–25. China: Guangzhow.

THEWS, J. G. & LANDWEBER, L. 1935 *U.S. Experimental Model Basin Rep.* 408. Washington, D.C.: Navy Yard.

THEWS, J. G. & LANDWEBER, L. 1936 *U.S. Experimental Model Basin Rep.* 414. Washington, D.C.: Navy Yard.

WHITHAM, G. B. 1965 *Proc. R. Soc. Lond.* A **283**, 238–261.

WHITHAM, G. B. 1974 *Linear and Nonlinear Waves*. Wiley.

WU, T. Y. 1979 *Tsunamis – Proc. National Science Foundation Workshop (May 7–9, 1979)*, pp. 110–149. Pasadena: Tetra Tech. Inc.

WU, T. Y. 1981 *J. Engng Mech. Div. ASCE* **107**, 501–522.

WU, T. Y. 1985 Keynote Lecture: On the generation of solitons. *Symp. on Fluid Mechanics Honoring Prof. C. S. Yih. 22–24 July 1985*. Michigan University, Ann Arbor, MI.

WU, T. Y. 1986 On generation of solitary waves by moving disturbances. *First Intern. Workshop on Water Waves and Floating Bodies. Feb. 16–19, 1986. MIT, Cambridge, MA.*

WU, T. Y. & WU, D. M. 1982 In *Proc. 14th Symp. on Naval Hydrodynamics*, pp. 103–125. Washington, D.C.: National Academy of Sciences.

WU, D. M. & WU, T. Y. 1987 Precursor solitons generated by three-dimensional disturbances moving in a channel. To be presented at *IUTAM Symp. on Non-linear Water Waves. August 25–28, 1987, Tokyo, Japan.*

ZHU, J. 1986 Internal solitons generated by moving disturbances. Ph.D. thesis. California Institute of Technology, Pasadena, CA.

ZHU, J., WU, T. Y. & YATES, G. T. 1986 Generation of internal runaway solitons by moving disturbances. *16th Symp. on Naval Hydrodynamics, July 14–18, 1986, University of California, Berkeley, CA.*

ZHU, J., WU, T. Y. & YATES, G. T. 1987 Internal solitary waves generated by moving disturbances. *Third Intl Symp. on Stratified Flows, February 3–5, 1987, California Institute of California, Pasadena, CA.*